DOI 10.1007/s10598-017-9369-y

Computational Mathematics and Modeling, Vol. 28, No. 3, July, 2017

NUMERICAL INVESTIGATION OF TRANSIENT FREE CONVECTIVE FLOW IN VERTICAL CHANNEL FILLED WITH POROUS MATERIAL IN THE PRESENCE OF THERMAL DISPERSION

Basant K. Jha[1] **and Babatunde Aina**[2]

The present work consists of a numerical investigation of transient free convective flow in vertical channel formed by two infinite vertical parallel plates filled with porous material in the presence of thermal dispersion. The governing coupled-nonlinear equations of momentum and energy transport are solved numerically using the implicit finite difference method, while the approximate analytical solution is also presented to find the expression for velocity, temperature, skin friction, and rate of heat transfer for the steady fully developed flow using the perturbation technique. The main objective is to investigate the effects of the dimensionless time, Darcy number, thermal dispersion, and Prandtl number on the fluid flow and heat transfer characteristics. Solutions are presented in graphical form and given in terms of fluid velocity, fluid temperature, skin friction, and rate of heat transfer for various parametric values. The significant result from this study is that velocity and temperature is enhanced with increase in thermal dispersion parameter and time. Furthermore, excellent agreement is found between the steady-state solution and the transient solution at large values of time.

Keywords: Transient Free Convective, Thermal Dispersion, Darcy number.

Nomenclacture

- C = thermal dispersion parameter
- C_ρ = specific heat of the fluid at constant pressure
- Da = Darcy number
- g = acceleration due to gravity
- Gr = Grashof number
- h = gap between the plates
- Nu_0 = Nusselt number at $Y = 0$
- Nu_1 = Nusselt number at $Y = 1$

Department of Mathematics, Ahmadu Bello University, Zaria, Nigeria.
[1] E-mail: basant777@yahoo.co.uk.
[2] E-mail: ainavicdydx@gmail.com (corresponding author).

 1046–283X/17/2803–0350

- Pr = Prandtl number
- t' = dimensional time
- t = dimensionless time
- T = temperature of the fluid
- T_0 = temperature of the fluid and plates in reference state $(t' \leq 0)$
- u' = dimensional velocity of the fluid
- U = dimensionless velocity of the fluid
- y' = dimensional coordinate perpendicular to the channel walls
- y = dimensionless coordinate perpendicular to the channel walls

Greek Letters

- β = coefficient of thermal expansion
- γ = ratio of kinematic viscosities
- θ = dimensionless temperature
- ρ = density
- τ_0 = dimensionless skin friction at $Y = 0$
- τ_1 = dimensionless skin friction at $Y = 1$
- v = fluid kinematic viscosity
- v_{eff} = effective kinematic viscosity
- k = thermal conductivity
- k_m = thermal conductivity of the solid phase
- k_f = thermal conductivity of the fluid phase

Introduction

Convective flow in a vertical channel filled with fluid-saturated porous materials has been attracting considerable attention recently as it plays a crucial role in various applications in contemporary technologies, such as the use of porous conical bearings in lubrication technology, packed-bed catalytic reactors, drying of porous

solids, waste disposal, storage of grain coal, petroleum industry, electronic cooling, high performance insulation for building and cold storage, aerodynamic heating, electrostatic precipitation, transport of heated and cooled fluid, and polymer technology, to mention a few. A number of studies on convective flow in vertical channel geometries filled with porous material have been undertaken by several researchers. Vafai and Tien [1] carried out a study on boundary and inertia effects on convective mass transfer in porous media. Srinivasen and Vafai [2] gave a theoretical analysis to investigate the solution for linear encroachment in two immiscible fluids in a porous medium. Vafai and Kim [3] used the Brinkman–Forcheimer extended Darcy model to obtain a closed form analytical solution for a fully developed flow in a porous channel subject to constant heat flux boundary conditions. Kaviany [4] studied laminar flow through a porous channel bounded by isothermal parallel plates, and they reported in their work that the Nusselt number for the fully developed flow increases with increase in the porous media shape parameter while Beckermann and Viskanta [5] conducted a theoretical investigation on forced convection boundary layer flow and heat transfer along a flat plate embedded in a porous medium. Also, Tien and Hunt [6] studied transport phenomenon for boundary layer flow and heat transfer in packed beds. Nakayama and Koyama [7] studied the more general case of free convection over a non-isothermal body of arbitrary shape embedded in a porous medium. Kou and Lu [8] studied mixed convection in a vertical channel embedded in a porous medium with asymmetric wall heat flux and found that reverse flow depends on the value of the mixed convection parameter. Rastogi and Poulikakos [9] examined the problem of double diffusive convection from a vertical plate in a porous medium saturated with a non-Newtonian power law fluid. Shenoy [10] presented many interesting applications of non-Newtonian power law fluids with yield stress on convective heat transport in fluid saturated porous media. Previous works investigated convective flow in a channel filled with porous material; these include the work of Pop and Ingham [11], Vafai [12], Nield and Began [13], and Bagchi and Kulacki [14].

On the other hand, Murthy and Singh [15] have reported on the effect of viscous dissipation on a non-Darcy natural convection boundary layer along an isothermal vertical wall embedded in a fluid saturated porous medium; in the case where inertia terms are prevalent, the thermal dispersion effects will become important. However, Hong and Tien [16] have analyzed the problem of thermal dispersion effects on natural convection about a heated horizontal cylinder in an enclosed porous medium. Hsiao et al. [17] discussed the influences of nonuniform porosity and thermal dispersion on natural convection about a heated horizontal cylinder in an enclosed porous medium. Moreover, Hsiao et al. [17] concluded that the effects of variable porosity and thermal dispersion increase the average Nusselt number and reduce the error between the experimentl data available and their solutions. Kuznetsov [18] presented an analytical study of the effect of transverse thermal dispersion on fully developed forced convection in a parallel plate channel filled with an isotropic fluid saturated porous medium. Meanwhile, Amiri and Vafai [19] suggested accounting for thermal dispersion by assuming that the effective thermal conductivity consists of both stagnant and dispersion conductivity. In their study, they constructed their correlation based on the experimental findings of Wakao and Kaguei [20]. Recently, Sheremet and Bachok [21] examined the effect of thermal dispersion on transient natural convection in a wavy-walled porous cavity filled with a nanofluid. From all the above discussed work, these effects were studied, and they have confirmed the importance of thermal dispersion effects studied in these papers.

Therefore, the objective of this study is to present a numerical analysis of transient free convective flow in vertical channel filled with porous material in the presence of thermal dispersion.

Mathematical Analysis

Consider a time dependent free convective flow in a vertical channel formed by two infinite vertical parallel plates filled with porous material in the presence of thermal dispersion. A schematic geometry of the problem

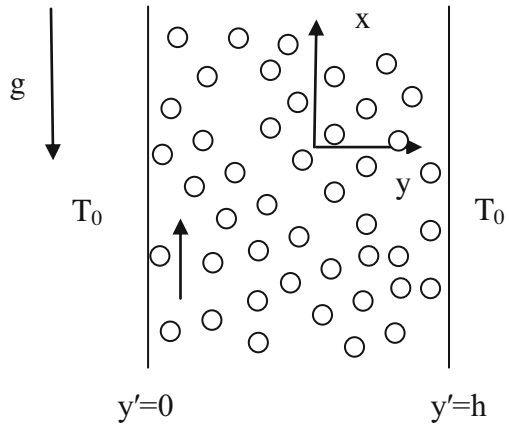

Fig. 1. Physical model and coordinate system.

under investigation is show in Fig. 1, where the x' axis is taken along one of the channel walls, and the y' axis is taken normal to the channel walls. Both channel walls are assumed to be separated by width h. At time $t' \le 0$, both channel walls are assumed to be at rest and the temperature of both channel walls and the fluid are assumed to be T_0. At time greater than zero, i.e. $t' > 0$, the temperature of the channel wall at $y' = 0$ is raised to T_w, causing free convection flow. In the present study, the following assumptions are made for the analysis:

I. The flow is assumed to be laminar, viscous and incompressible

II. The flow is assumed to be fully developed both hydrodynamically and thermally and hence there is no property variation in axial direction.

Therefore, under these assumptions, along with the Boussinesq's approximation, the governing equations of momentum and energy balance that describe the present physical situation in dimensional form are

$$\frac{\partial u'}{\partial t'} = \nu_{\text{eff}} \frac{\partial^2 u'}{\partial y'^2} + g\beta(T - T_0) - \frac{\nu}{K} u', \tag{1}$$

$$\frac{\partial T'}{\partial t'} = \frac{k_f}{\rho C_\rho} \frac{\partial}{\partial y'} \left[\left(\frac{k_m}{k_f} + C \,\text{Pr} \frac{u'}{\nu} dp \right) \frac{\partial T'}{\partial y'} \right] \tag{2}$$

subject to the corresponding initial and boundary condition to be satisfied

$$\begin{aligned} &u' = 0, \quad T' = T_0 \quad \text{for} \quad 0 \le y' \le h \quad \text{at} \quad t' \le 0, \\ &u' = 0, \quad T' = T_w, \quad \text{when} \quad y' = 0 \quad \text{at} \quad t' > 0, \\ &u' = 0, \quad T' = T_0, \quad \text{when} \quad y' = h \quad \text{at} \quad t' > 0. \end{aligned} \tag{3}$$

We introduce the following dimensionless quantities in Eqs. (1)–(3)

$$t = \frac{t'\nu}{h^2}, \quad y = \frac{y'}{h}, \quad U = \frac{u'}{u_0}, \quad \theta = \frac{T' - T_0}{T_w - T_0}, \quad u_0 = \frac{g\beta(T_w - T_0)h^2}{\nu}, \tag{4}$$

$$\Pr = \frac{C_p\mu}{k}, \quad \gamma = \frac{\nu_{\text{eff}}}{\nu}, \quad Da = \frac{k}{h^2}, \quad kr = \frac{k_m}{k_f}, \quad Gr = \frac{u_0 dp}{\nu}.$$

Substituting Eq. (4) into Eqs. (1)–(3), we obtain the following dimensionless momentum and energy equations

$$\frac{\partial U}{\partial t} = \gamma \frac{\partial^2 U}{\partial y^2} + \theta - \frac{U}{Da}, \tag{5}$$

$$\frac{\partial \theta}{\partial t} = \frac{1}{\Pr}\frac{k_m}{k_f}\frac{\partial^2 \theta}{\partial y^2} + GrC\,\frac{\partial}{\partial y}\left(U\frac{\partial \theta}{\partial y}\right). \tag{6}$$

The corresponding initial and boundary conditions for these equations in dimensionless form are given by

$$\begin{aligned} &U = 0, \quad \theta = 0, \quad \text{for} \quad 0 \le y \le 1 \quad \text{at} \quad t \le 0, \\ &U = 0, \quad \theta = 1, \quad \text{when} \quad y = 0 \quad \text{at} \quad t > 0, \\ &U = 0, \quad \theta = 0, \quad \text{when} \quad y = 1 \quad \text{at} \quad t > 0. \end{aligned} \tag{7}$$

The physical quantities used in the above equations are defined in the nomenclature.

Analytical Solution

The governing equations presented in the previous section are highly nonlinear and coupled due to the presence of thermal dispersion and exhibit no analytical solutions. Analytical solutions, on the other hand, are very important for many reasons. They provide a standard for checking the accuracies of many approximate methods such as numerical or empirical. It is well know that analytical solutions have their own theoretical meaning, and many analytical solutions played key roles in the early development of fluid mechanics and heat conduction. Besides their theoretical meaning, analytical solutions can also be applied to checking the accuracy, convergence, and effectiveness of various numerical computation methods and improving differencing schemes, grid generation methods and so on. Analytical solutions are therefore very useful even for the newly rapidly developing computational fluid dynamics and heat transfer. It is, therefore, of interest to reduce the governing equations of the present problem to a form that can be solved analytically. A special case of the present problems that exhibits analytical solution is the problem of steady free convection flow in a vertical channel filled with porous material in the presence of thermal dispersion. The resulting steady-state equations and boundary conditions can be written as

$$\gamma \frac{d^2U}{dy^2} - \frac{U}{Da} + \theta = 0, \tag{8}$$

$$\frac{k_m}{k_f} \frac{d^2\theta}{dy^2} + Gr \Pr C \frac{d}{dy}\left(U \frac{d\theta}{dy} \right) = 0, \tag{9}$$

The boundary conditions are

$$U = 0, \quad \theta = 1, \quad \text{at} \quad y = 0, \tag{10}$$

$$U = 0, \quad \theta = 0, \quad \text{at} \quad y = 1.$$

In order to construct an analytical solution of Eqs. (8) and (9), subject to the boundary conditions in Eq. (10), we employed a regular perturbation method by taking a power series expansion in the thermal dispersion parameter C such as

$$U(y) = U_0(y) + \varepsilon U_1(y) + \varepsilon^2 U_2(y) + \ldots = \sum_{i=0}^{\infty} \varepsilon^i U_i(y), \tag{11}$$

$$\theta(y) = \theta_0(y) + \varepsilon \theta_1(y) + \varepsilon^2 \theta_2(y) + \ldots = \sum_{i=0}^{\infty} \varepsilon^i \theta_i(y), \tag{12}$$

where $\varepsilon = Gr * \Pr * C$ is the perturbation parameter $(\varepsilon << 1)$. The first and higher order terms of ε give a correction to U_0, θ_0 accounting for the thermal dispersion effect. Substituting Eqs. (11) and (12) into Eqs. (8) and (9) and equating like powers of ε, one obtains the boundary value problems for $i = 0$ and $i = 1$ as

$$\gamma \frac{d^2U_0}{dy^2} - \frac{U_0}{Da} + \theta_0 = 0, \tag{13}$$

$$\frac{k_m}{k_f} \frac{d^2\theta_0}{dy'} = 0, \tag{14}$$

$$\gamma \frac{d^2U_1}{dy^2} - \frac{U_1}{Da} + \theta_1 = 0, \tag{15}$$

$$\frac{k_m}{k_f} \frac{d^2\theta_1}{dy^2} + Gr \Pr \frac{d}{dy}\left(U_0 \frac{d\theta_0}{dy} \right) = 0. \tag{16}$$

The boundary conditions to be satisfied are

$$U_0 = U_1 = \theta_1 = 0, \quad \theta_0 = 1, \quad \text{at} \quad y = 0, \tag{17}$$

$$U_0 = U_1 = \theta_0 = \theta_1 = 0 \quad \text{at} \quad y = 1.$$

The solutions of Eqs. (13) to (16) subject to boundary conditions (17) are

$$U(y) = U_0(y) + \varepsilon U_1(y), \tag{18}$$

where

$$U_0(y) = Da\,\frac{\sinh\left(\frac{y-1}{\sqrt{\gamma Da}}\right)}{\sinh\left(\frac{1}{\sqrt{\gamma Da}}\right)} + (1-y)\,Da,$$

$$U_1(y) = \left[\frac{Gr\,\mathrm{Pr}\,Da^3}{kr} - \frac{A_2 Da}{kr}\right]\frac{\sinh\left(\frac{(1-y)}{\sqrt{\gamma Da}}\right)}{\sinh\left(\frac{1}{\sqrt{\gamma Da}}\right)} + \frac{Gr\,\mathrm{Pr}\,Da^3}{kr}\left[\frac{\sinh\left(\frac{y}{\sqrt{\gamma Da}}\right)}{\sinh\left(\frac{1}{\sqrt{\gamma Da}}\right)} - 1\right]$$

$$+ \frac{Gr\,\mathrm{Pr}\,Da^2}{2kr}\left[\frac{\sinh\left(\frac{y}{\sqrt{\gamma Da}}\right)}{\sinh\left(\frac{1}{\sqrt{\gamma Da}}\right)} - y^2\right] - \left[\frac{yGr\,\mathrm{Pr}\,Da^2}{2kr}\right]\frac{\sinh\left(\frac{(y-1)}{\sqrt{\gamma Da}}\right)}{\sinh\left(\frac{1}{\sqrt{\gamma Da}}\right)}$$

$$+ \frac{Da\,[A_1 y + A_2]}{kr} - \frac{\sinh\left(\frac{y}{\sqrt{\gamma Da}}\right)}{\sinh\left(\frac{1}{\sqrt{\gamma Da}}\right)}\frac{[A_1 + A_2]\,Da}{kr},$$

$$\theta(y) = \theta_0(y) + \varepsilon\theta_1(y), \tag{19}$$

where

$$\theta_0(y) = 1 - y,$$

$$\theta_1(y) = \left[\frac{Gr\,\mathrm{Pr}\,Da\sqrt{\gamma Da}}{kr}\right]\frac{\cosh\left(\frac{y-1}{\sqrt{\gamma Da}}\right)}{\sinh\left(\frac{1}{\sqrt{\gamma Da}}\right)} - \frac{Gr\,\mathrm{Pr}\,Da}{kr}\frac{y^2}{2} + \frac{A_1 y}{kr} + \frac{A_2}{kr},$$

$$A_1 = \frac{Gr\,\mathrm{Pr}\,Da}{kr} + \frac{Gr\,\mathrm{Pr}\,Da\sqrt{\gamma Da}}{kr\sinh\left(\frac{1}{\sqrt{\gamma Da}}\right)}\left[\cosh\left(\frac{1}{\sqrt{\gamma Da}}\right) - 1\right], \qquad A_2 = -\frac{Gr\,\mathrm{Pr}\,Da\sqrt{\gamma Da}}{kr}\left[\frac{\cosh\left(\frac{1}{\sqrt{\gamma Da}}\right)}{\sinh\left(\frac{1}{\sqrt{\gamma Da}}\right)}\right].$$

Using (18), we write the steady-state skin frictions on the boundaries

$$\tau_0 = \left.\frac{dU}{dy}\right|_{y=0} = \left.\frac{dU_0}{dy}\right|_{y=0} + \varepsilon \left.\frac{dU_1}{dy}\right|_{y=0}, \tag{20}$$

$$\tau_1 = \left.\frac{dU}{dy}\right|_{y=1} = \left.\frac{dU_0}{dy}\right|_{y=1} + \varepsilon \left.\frac{dU_1}{dy}\right|_{y=1}. \tag{21}$$

Also, the steady-state rate of heat transfer on the boundaries are

$$Nu_0 = \left.\frac{d\theta}{dy}\right|_{y=0} = -1 + \varepsilon\left[\frac{A_1}{kr} - \frac{Gr\,\mathrm{Pr}\,Da}{kr}\right], \tag{22}$$

$$Nu_1 = \left.\frac{d\theta}{dy}\right|_{y=1} = -1 + \varepsilon\left[\frac{A_1}{kr} - \frac{Gr\,\mathrm{Pr}\,Da}{kr}\right]. \tag{23}$$

In the following section, Eqs. (5)–(7) are solved numerically and the skin friction together with the rate of heat transfer are computed.

Numerical Solution

The momentum and energy equations given by Eqs. (5) and (6) are solved numerically by using the implicit finite difference method. The procedure involves discretization of the transport equations (5) and (6) into the finite difference equations at the grid point (i, j). They are, in order, as follows:

$$\frac{U(i,j) - U(i,j-1)}{\Delta t} = \gamma\left[\frac{U(i+1,j) - 2U(i,j) + U(i-1,j)}{(\Delta y)^2}\right] - \frac{U(i,j)}{Da} + \theta(i,j), \tag{24}$$

$$\frac{\theta(i,j) - \theta(i,j-1)}{\Delta t} = \frac{1}{\mathrm{Pr}}\frac{k_m}{k_f}\left[\frac{\theta(i+1,j) - 2\theta(i,j) + \theta(i-1,j)}{(\Delta y)^2}\right] + GrC\left[U(i,j)\left\{\frac{\theta(i+1,j) - \theta(i-1,j)}{2\Delta y}\right\}\right]. \tag{25}$$

The time derivative is replaced by the backward difference formula, while spatial derivative is replaced by the central difference formula. The above equations are solved by the Thomas algorithm by manipulating them into a system of linear algebraic equations in the tridiagonal form. In each time step, the process of numerical integration for every dependent variable starts from the first neighboring grid point of the channel wall at $y = 0$ and using the tridiagonal form of the finite difference equation (5) and (6) until it reaches the immediate grid point

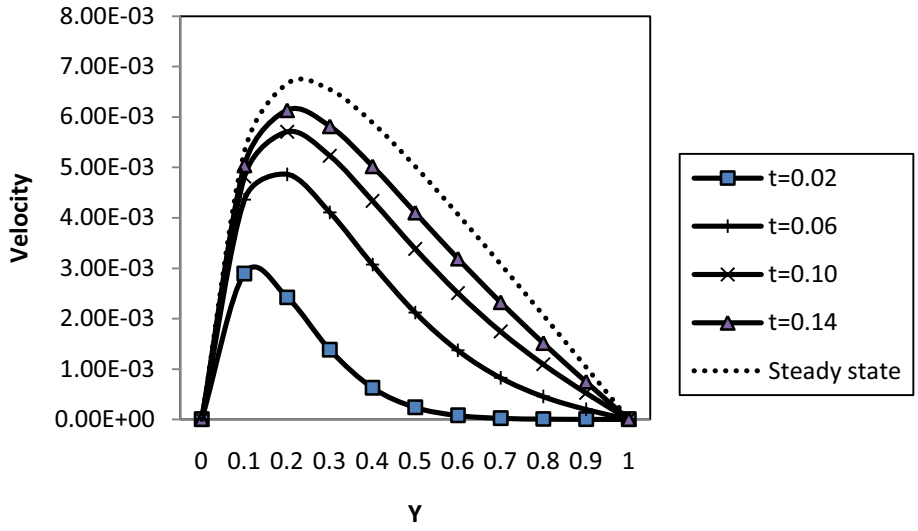

Fig. 2a. Velocity profile for transient and steady state $(Da = 0.01, C = 0.2, \Pr = 0.71, Gr = 100)$.

of the channel wall at $y = 1$. In each time step the temperature field has been solved, and the evaluated values are used to obtain the velocity field. The process of computation is advanced until a steady state is approached that satisfies the following convergence criterion:

$$\frac{\sum \left| A_{i,j+1} - A_{i,j} \right|}{M \left| A \right|_{\max}} < 10^{-4} \tag{26}$$

with respect to the temperature and velocity fields; here, $A_{i,j}$ stands for the velocity and temperature fields, M is the number of interior grid points, and $\left| A \right|_{\max}$ is the maximum absolute value of $A_{i,j}$.

In the numerical computation, there is a need to specify Δt to get a steady solution as rapidly as possible, yet small enough to avoid instabilities. It is set, suitable for the present computation, as

$$\Delta t = \text{stabr} \times (\Delta y)^2.$$

The parameter stabr is determined by numerical experiment in order to achieve convergence and stability of the solution procedure. Numerical experiments show that the value 2 is suitable for numerical computations. In order to confirm the validity of this numerical model, the numerical results are compared with the analytical solution derived for the steady-state problem using the perturbation technique. At large values of time, the obtained numerical values using the implicit finite difference method for velocity, temperature, skin-friction, and rate of heat transfer are in excellent agreement with the obtained steady-state values using the perturbation method.

Results and Discussion

The governing coupled-nonlinear equations of momentum and energy transport are solved numerically by using the implicit finite difference method, and in order to verify the validity of the adopted numerical scheme,

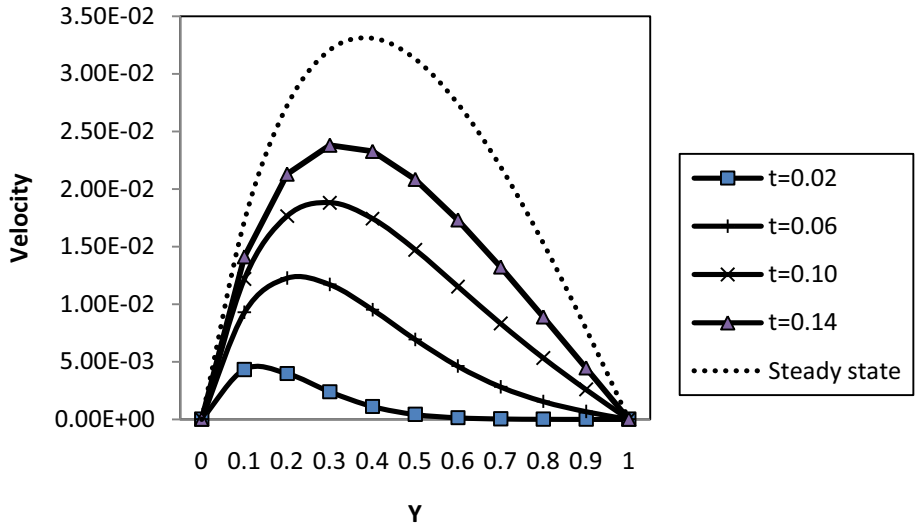

Fig. 2b. Velocity profile for transient and steady state $(Da = 0.1, C = 0.2, \Pr = 0.71, Gr = 100)$.

the steady-state versions of Eqs. (5)–(7) are solved analytically by using the perturbation technique. The effects of governing physical parameters, such as Prandtl number $(\Pr)$, which is inversely proportional to the thermal diffusivity of the working fluid, the non-dimensional time (t), Darcy number (Da), and thermal dispersion parameter (C) on the flow formation are reported in this section. This study has been performed over the reasonable ranges of

$$0.01 < Da < 0.1, \quad 0.0 < t < 0.6, \quad \text{and} \quad 0.0 < C < 0.5.$$

The selected reference values of Da, t, and C for the present analysis are 0.1, 0.2 and 0.2, respectively.

Figure 2 exhibits the effects of the Darcy number (Da) and nondimensional time (t) on the transient velocity profiles for fixed values of thermal dispersion parameter $(C = 0.2)$ and the Prandtl number $(\Pr = 0.71)$. It is clearly seen in Fig. 2 that increase in the Darcy number leads to enhancement in fluid velocity for both transient and steady state. Furthermore, by increasing the nondimensional time, the fluid velocity increases. This is a consequence of the temperature increase that results from increase in time, since the convection current becomes stronger and hence velocity increases with time. Also, the velocity is observed to attain a steady state while the time required to reach steady state increases as the Darcy number increase.

Figure 3 depicts the combined effects of Darcy number (Da) and nondimensional time (t) on the transient temperature profiles for fixed values of thermal dispersion parameter $(C = 0.2)$ and Prandtl number $(\Pr = 0.71)$. It shows that temperature increases with increase in time, finally attaining its steady state.

Figures 4 and 5 exhibit the effects of Prandtl number $(\Pr)$ and Darcy number (Da) on the velocity and temperature profiles, respectively, for fixed values of thermal dispersion parameter $(C = 0.2)$ and time $(t = 0.2)$. It is clearly shown in these figures that the fluid velocity and temperature decrease as the Prandtl number increases. The physical explanation is that, fluids with high Prandtl number have a lower thermal conductivity and high viscosity, which causes low heat penetration and reduces the thermal boundary layer. Furthermore, by increasing the Darcy number, the fluid velocity and temperature increases.

Figures 6 and 7 illustrate the influences of thermal dispersion parameter (C) and Darcy number (Da) on the velocity and temperature profiles, respectively, for fixed values of the Prandtl number $(\Pr = 0.71)$ and

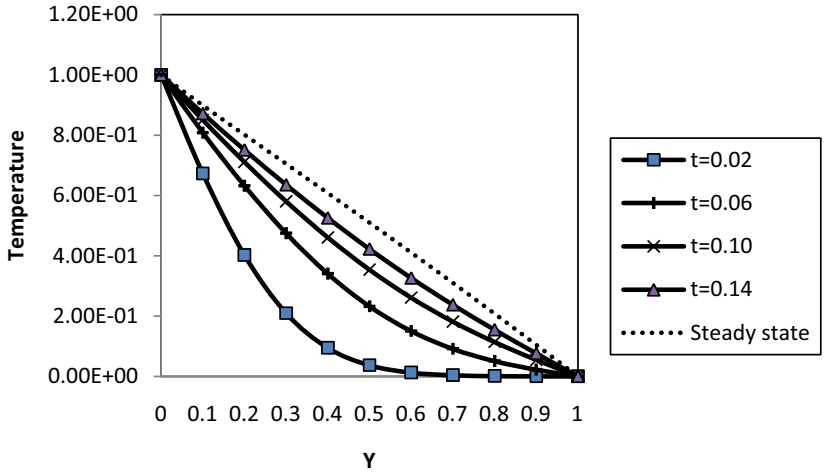

Fig. 3a. Temperature profile for transient and steady state $(Da = 0.01, C = 0.2, \Pr = 0.71, Gr = 100)$.

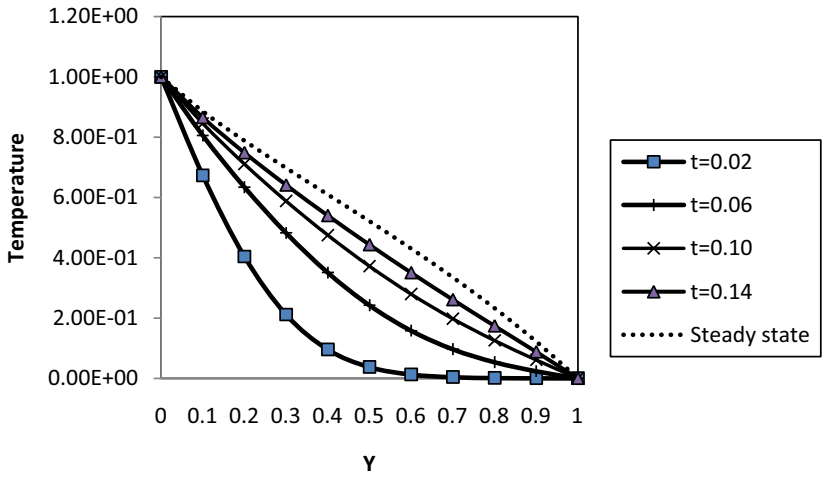

Fig. 3b. Temperature profile for transient and steady state $(Da = 0.1, C = 0.2, \Pr = 0.71, Gr = 100)$.

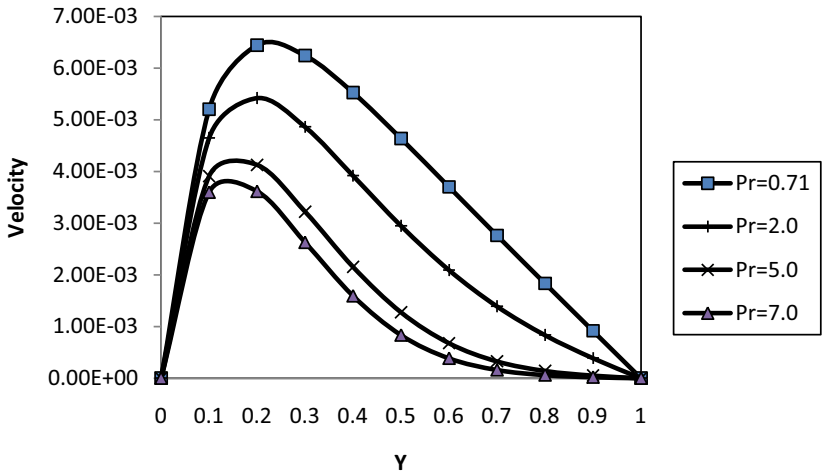

Fig. 4a. Velocity profile for different values of Prandtl number $(Da = 0.01, Gr = 100, C = 0.2, t = 0.2)$.

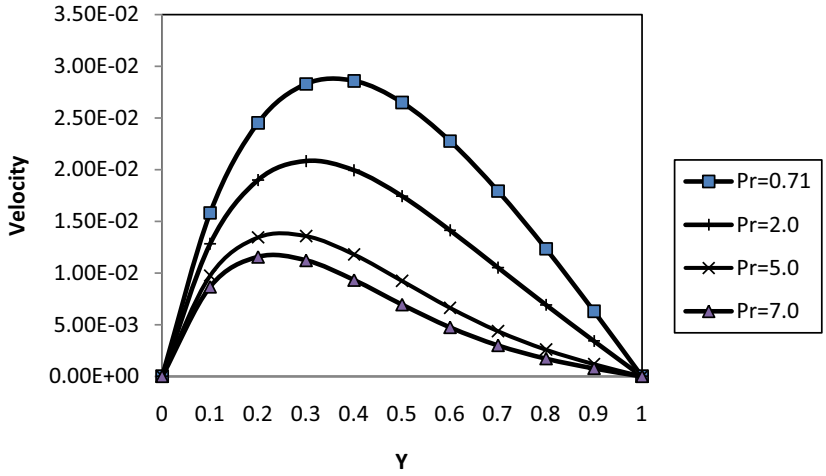

Fig. 4b. Velocity profile for different values of Prandtl number $(Da = 0.1, Gr = 100, C = 0.2, t = 0.2)$.

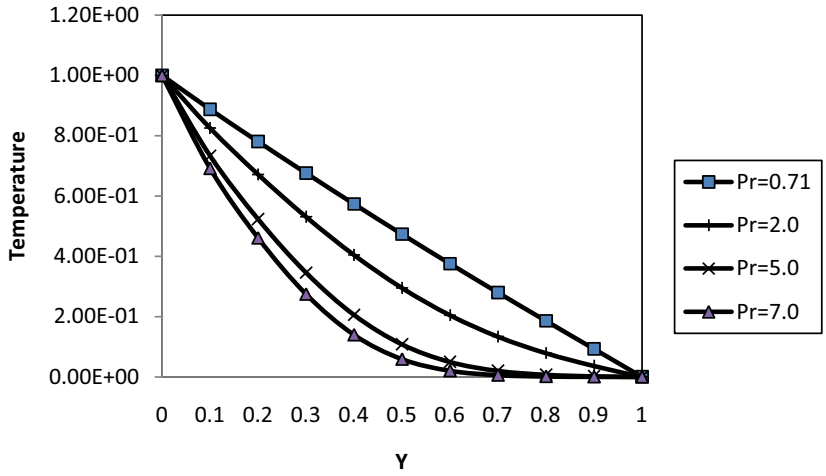

Fig. 5a. Temperature profile for different values of Prandtl number $(Da = 0.01, Gr = 100, C = 0.2, t = 0.2)$.

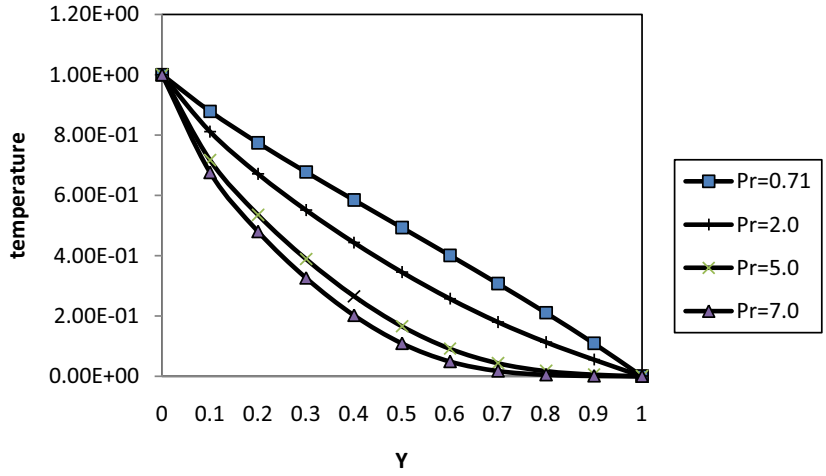

Fig. 5b. Temperature profile for different values of Prandtl number $(Da = 0.1, Gr = 100, C = 0.2, t = 0.2)$.

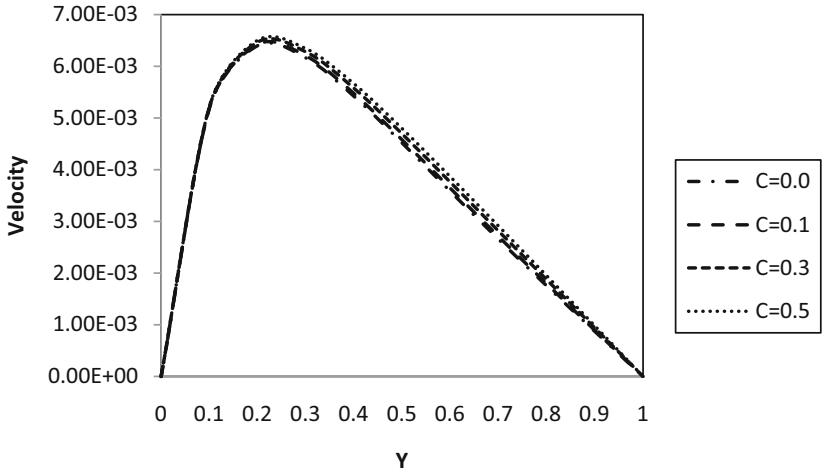

Fig. 6a. Velocity profile for different values of C $(Da = 0.01, Gr = 100, \Pr = 0.71, t = 0.2)$.

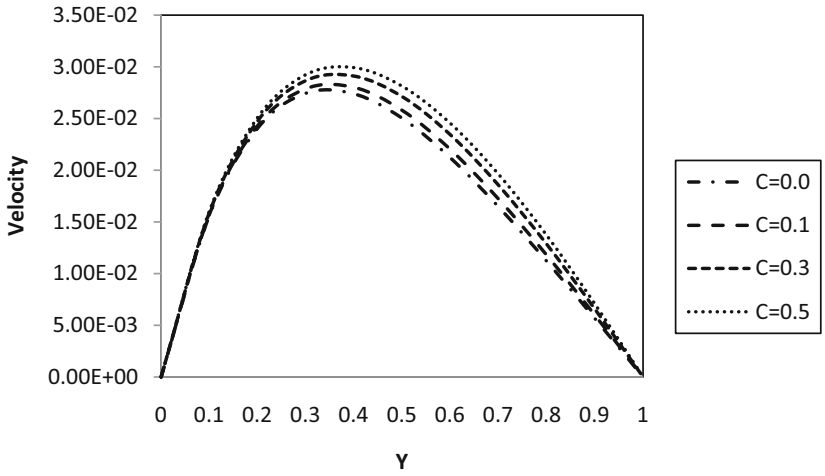

Fig. 6b. Velocity profile for different values of C $(Da = 0.1, Gr = 100, \Pr = 0.71, t = 0.2)$.

time $(t = 0.2)$. It is found that the fluid velocity and temperature increase with increase in the thermal dispersion parameter. This is physically true because an increase in thermal dispersion adds more heat to the fluid, leading to an increase in temperature, which causes a velocity increase. Furthermore, it is interesting to note from these figures that the impact of the thermal dispersion parameter on the fluid velocity and temperature is more pronounced for higher values of the Darcy number.

Figure 8 exhibit the effects of nondimensional time (t) and thermal dispersion (C) on the skin friction at the channel walls. The figure reveals that, as the thermal dispersion parameter increases, the skin friction increases. This is evident from the increase in velocity gradient that results from the increase in thermal dispersion parameter. In addition, the skin friction is observed to increase with increase in time on both channel walls and attains a steady state at large values of time.

Figure 9 reveals the effects of thermal dispersion parameter (C) and nondimensional time (t) on the rate of heat transfer at the channel walls. It is evident that as the thermal dispersion parameter increases the rate of heat transfer increases. This is attributed to the fact that, increase in thermal dispersion parameter increase the fluid velocity. Consequently, the temperature gradient increase leads to an increase in the rate of heat transfer

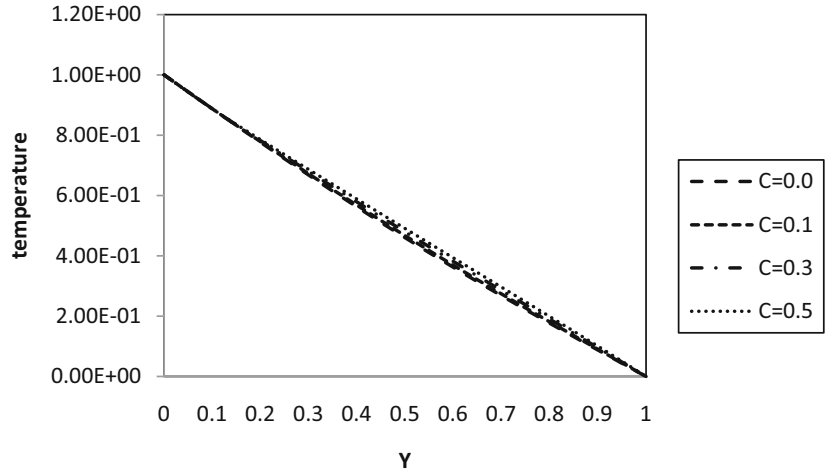

Fig. 7a. Temperature profile for different values of C $(Da = 0.01, Gr = 100, \Pr = 0.71, t = 0.2)$.

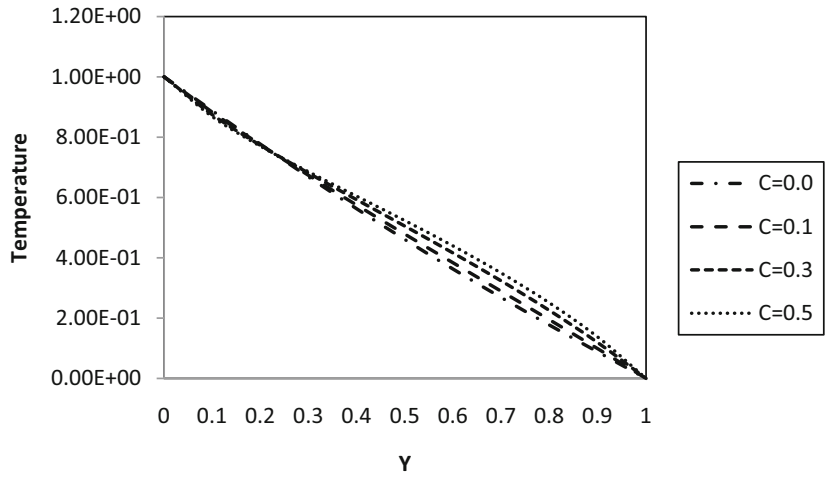

Fig. 7b. Temperature profile for different values of C $(Da = 0.1, Gr = 100, \Pr = 0.71, t = 0.2)$.

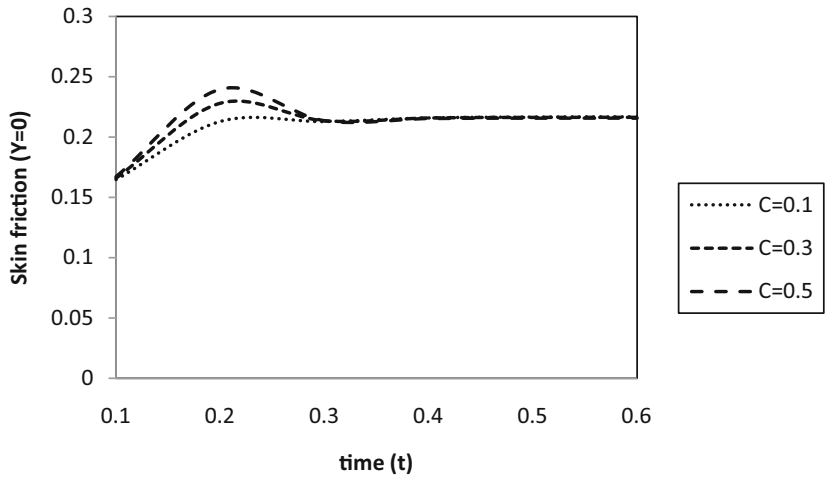

Fig. 8a. Variation of skin friction versus time (t) for different values of C at $(y = 0)$.

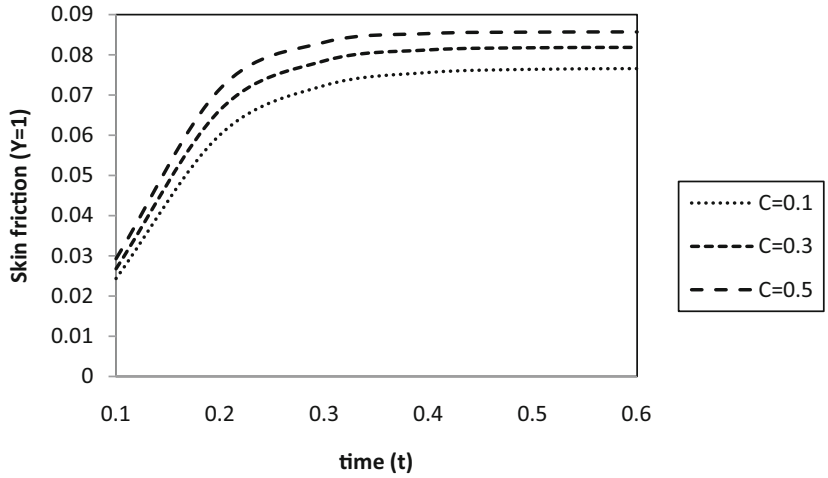

Fig. 8b. Variation of skin friction versus time (t) for different values of C at $(y=1)$.

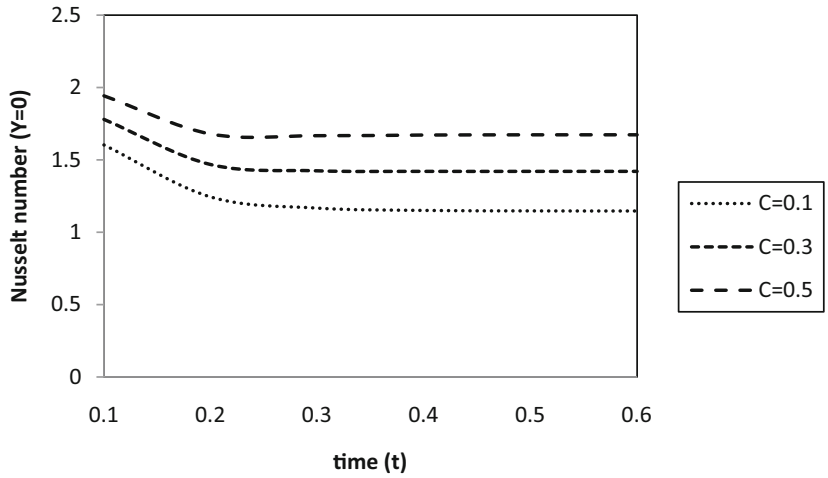

Fig. 9a. Variation of Nusselt number versus time (t) for different values of C at $(y=0)$.

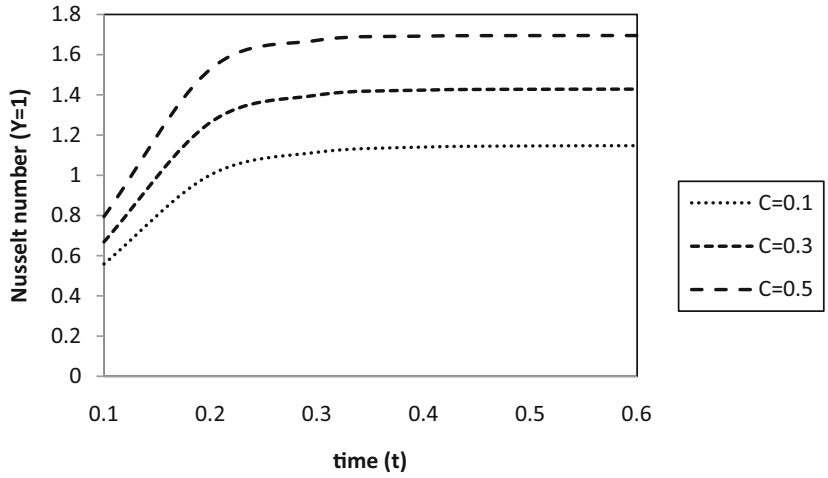

Fig. 9b. Variation of Nusselt number versus time (t) for different values of C at $(y=1)$.

Table 1. Comparison of Numerical Value of the Transient State Velocity Obtained Using the Implicit Finite Difference and the Steady State Velocity Obtained Analytically

y	Velocity $(kr = 1.0, \mathrm{Pr} = 0.71, Gr = 10, C = 0.02, Da = 0.1, t = 0.6)$	
	Implicit Finite Difference	Perturbation Method
0.0	0.00000000	0.00000000
0.1	0.01721498	0.01722647
0.2	0.02709612	0.02711623
0.3	0.03164869	0.03167474
0.4	0.03233948	0.03236880
0.5	0.03024531	0.03027518
0.6	0.02616186	0.02618963
0.7	0.02068426	0.02070752
0.8	0.01426731	0.01428403
0.9	0.00727159	0.00728034
1.0	0.00000000	0.00000000

on the channel walls. Furthermore, it is found that, at large values of time, the rate of heat transfer attains a steady-state value.

Finally, in order to see the accuracy of the numerical solutions, numerical values of velocity and temperature are presented in Tables 1 and 2, respectively, for steady-state operating conditions using the perturbation technique and the implicit finite difference method for the transient mathematical model. It is evident from these tables that, for large values of nondimensional time $(t = 0.6)$, the steady-state and transient solutions are in excellent agreement. This comparison inspires confidence in the numerical solutions and shows that the numerical method is adequate for the solutions of the present study.

CONCLUSIONS

Numerical as well as analytical solutions are derived for transient and steady free convective flow in a vertical channel formed by two infinite vertical parallel plates filled with porous material in the presence of thermal dispersion. The temperature field and velocity field are obtained analytically by the perturbation method for steady-free convection flow in a vertical channel and numerically by the implicit finite difference technique for transient free convective flow in a vertical channel. Graphical results for the temperature, velocity, skin friction, and rate of heat transfer are presented and discussed for various physical parameter values. The main

Table 2. Comparison of Numerical Value of the Transient State Temperature Obtained Using the Implicit Finite Difference and the Steady State Temperature Obtained Analytically

y	Temperature $(kr = 1.0, \mathrm{Pr} = 0.71, Gr = 10, C = 0.02, Da = 0.1, t = 0.6)$	
	Implicit Finite Difference	Perturbation Method
0.0	1.00000000	1.00000000
0.1	0.89978640	0.89983499
0.2	0.79976770	0.79985975
0.3	0.69985820	0.69998502
0.4	0.59999650	0.60014605
0.5	0.50013830	0.50029600
0.6	0.40025100	0.40040123
0.7	0.30031010	0.30043791
0.8	0.20029670	0.20038960
0.9	0.10019680	0.10024563
1.0	0.00000000	0.00000000

findings are as follows:

I. It is found that increase in the thermal dispersion parameter and time enhances the skin friction and rate of heat transfer.

II. The time required to reach steady state velocity and temperature field is strongly dependent on the Prandtl number and thermal dispersion parameter.

III. The impact of the thermal dispersion parameter on the fluid velocity and temperature is more pronounced for higher values of the Darcy number.

REFERENCES

1, K. Vafai and C. L. Tien, "Boundary and inertia effects on convective mass transfer in porous media," *Int. J. Heat Mass Trans.,* **25**, 1183–1190 (1982).

2, V. Srinivasan and K. Vafai, "Analysis of linear encroachment in two-immiscible fluid systems in a porous medium," *ASME J. Fluids Eng*., **116**, 135–139 (1994).

3. K. Vafai and S. J. Kim, "Forced convection in a channel filled with a porous medium: An exact solution," *ASME J. Heat Transf*., **111**, 1103–1106 (1989).

4. M. Kaviany, *Principles of Heat Transfer in Porous Media,* 2nd ed. Springer, New York (1995).
5. C. Beckermann and R. Viskanta, "Forced convection boundary layer flow and heat transfer along a flat plate embedded in a porous medium," *Int. J. Heat Mass Transf.* **30**, 1547–1551 (1987).
6. C. L. Tien and M. L. Hunt, "Boundary layer flow and heat transfer in porous beds," *Chem. Eng.: Process Intensif.*, **21**, No. 1, 53–63 (1987).
7. A. Nakayama and H. Koyama, "Buoyancy induced flow of non-Newtonian fluids over a non isothermal body of arbitrary shape in a fluid-saturated porous medium," *Appl. Sci. Res.,* **48**, 55–70 (1991).
8. H. S. Kou and K. T. Lu, "The analytical solution of mixed convection in a vertical channel embedded in a porous media with asymmetric wall heat fluxes," *Int. J. Heat Mass Transf.,* **20**, 737–750 (1993).
9. S. K. Rostagi and D. Poulikakos, "Double diffusion from a vertical surface in a porous region saturated with a non-Newtonian fluid," *Int. J. Heat Mass Transf.*, **38**, 935–946 (1995).
10. A.V. Shenoy, "Non-Newtonian fluid heat transfer in a porous media," in: *Advances in Heat Transfer*, **24**, Academic Press, New York (1994), pp. 101–190.
11. I. Pop and D. B. Ingham, *Convective Heat Transfer: Mathematical and Computational Modeling of Viscous Fluids and Porous Media,* Pergamon, Oxford (2001).
12. K. Vafai, *Porous Media: Applications in Biological Systems and Biotechnology,* CRC Press, Tokyo (2010).
13. D. A. Nield and A. Bejan, *Convection in Porous Media,* 4th ed., Springer, New York (2013).
14. A. Bagchi and F. A. Kulacki, *Natural Convection in Superposed Fluid-Porous Layers,* Springer, New York (2014).
15. P.V.S.N Murthy and P. Singh, "Effect of viscous dissipation on a non-Darcy natural convection regime," *Int. J. Heat Mass Transf.*, **40**, 1251–1260 (1997) .
16. J. T. Hong and C. L. Tien, "Analysis of thermal dispersion effect on vertical-plate natural convection in porous media," *Int. J. Heat Mass Transf.,* **30**, 143–150 (1987).
17. S. W. Hsiao, P. Cheng and C. K. Chen, "Non-uniform porosity and thermal dispersion effects on natural convection about a heated horizontal cylinder in an enclosed porous medium," *Int. J. Heat Mass Transf.,* **35**, 3407-3418 (1992).
18. A. V. Kuznetsov, "Influence of thermal dispersion on forced convection in a composite parallel-plate channel," *Z. Angew. Math. Phys.,* **52**, 135–150 (2001).
19. A. Amiri and K. Vafai, "Analysis of dispersion effects and non-thermal equilibrium, non-Darcian, variable porosity, incompressible flow through porous media," *Int. J. Heat Mass Transf.*, **37**, 939–954 (1994).
20. N. Wakao and S. Kaguei, *Heat and Mass Transfer in Packed Beds,* Gordon and Breach, New York (1996).
21. M. A. Sheremet, I. Pop, and N. Bachok, "Effect of thermal dispersion on transient natural convection in a wavy-walled porous cavity filled with a nanofluid: Tiwari and Das nanofluid model," *Int. J. Heat Mass Transf.*, **92**, 1053–1060 (2016).